J|A|C|S
ARTICLES
Published on Web 05/17/2006

Lariatins, Antimycobacterial Peptides Produced by *Rhodococcus* sp. K01−B0171, Have a Lasso Structure

Masato Iwatsuki,[†] Hiroshi Tomoda,[‡] Ryuji Uchida,[†] Hiroaki Gouda,[‡] Shuichi Hirono,*[,‡] and Satoshi Ōmura*[,†]

Contribution from the Kitasato Institute, and the Kitasato Institute for Life Sciences, Kitasato University, Minato-ku, Tokyo 108, Japan, and School of Pharmaceutical Sciences, Kitasato University, Minato-ku, Tokyo 108, Japan

Received October 11, 2005; E-mail: hironos@pharm.kitasato-u.ac.jp; omura-s@kitasato.or.jp

Abstract: Two antimycobacterial agents, lariatins A and B, were isolated from the culture broth of *Rhodococcus* sp. K01−B0171. Their structures were elucidated by spectral analysis and advanced protein chemical methods to be unique cyclic peptides, which consist of 18 and 20 L-amino acid residues with an internal linkage between the γ-carboxyl group of Glu8 and the α-amino group of Gly1. The three-dimensional structure of lariatin A deduced from NMR data by dynamical simulated annealing method indicates that the tail segment (Trp9-Pro18) passes through the ring segment (Gly1-Glu8) to form a 'lasso' structure.

Introduction

Tuberculosis (TB) is still the greatest single infectious cause of mortality in the world, together with HIV and malaria.[1] Moreover, the spread of HIV has increased the number of tuberculosis patients.[2] However, powerful anti-TB drugs with a new mechanism of action have not been developed in over 30 years, and only 5 antituberculous drugs can still be used clinically. While screening for microbial metabolites showing specific inhibitory activity against *Mycobacterium smegmatis*,[3] we discovered the novel agents designated lariatins A and B, unique cyclic peptides produced by *Rhodococcus* sp. K01−B0171 (Figure 1). They showed selective activity against *M. smegmatis* with MIC values of 3.13 and 6.25 μg/mL, respectively, and also inhibited the growth of *M. tuberculosis*. In this paper, we show that they consist of 18 and 20 amino acid residues with an internal linkage between the γ-carboxyl group of Glu8 and the α-amino group of Gly1. Furthermore, we show that lariatin A is folded into a 'lasso' structure.

Results

Structure Elucidation. After centrifugation of the 4-day old culture broth (16 L), the supernatant was separated by HP-20, ODS, and LH-20 column chromatography and reversed-phase HPLC to afford lariatins A (**1**, 38.2 mg) and B (**2**, 11.2 mg) as pale yellow powders.

Lariatin A (**1**) had a molecular formula $C_{94}H_{144}N_{27}O_{25}$ established on the basis of NMR and HRFABMS 2051.0764 $[M+H]^+$ (calcd 2051.0826). The Rydon-Smith reaction was positive and the absorption at 1655 cm^{-1} was dominant in the IR spectrum, indicating that this compound is a peptide. The ^{13}C NMR spectrum contained 18 carbonyl signals near δ 171, and 18 methine signals between δ 55 and 63, typical for a peptide. The ^1H NMR spectrum contained signals for α-protons of the amino acid residues. The complete acid hydrolysis of lariatin A and ^1H NMR spectrum indicated an amino acid content as follows: 1 Asx, 2 Glx, 2 Ser, 2 Gly, 1 His, 1 Arg, 1 Pro, 1 Tyr, 3 Val, 1 Ile, 1 Leu, 1 Lys, 1 Trp. The MS/MS analysis revealed that the partial sequence of the C-terminal side is Trp-Val-Gly-His-Ser-Asn-Val-Ile/Leu-Lys/Glu-Pro. The presence of Asn shows that 2 Glx should be 1 Gln and 1 Glu from the molecular weight. Therefore, the MW of lariatin A corresponds to its amino acid composition minus the weight of one water molecule, indicating that the molecule must be cyclized. A detailed analysis of ^1H-^{13}C HMBC and NOESY spectral data revealed some partial sequences such as Gly-Ser-Glx, Leu-Val-Tyr-Arg-Glx, Trp-Val-Gly, Ser-Asn, and Val-Ile-Lys-Pro. An N-terminal sequence analysis was performed using automated Edman degradation but did not yield any amino acid sequence information, indicating that the terminal α-amino group was modified. This result also suggested that the molecule is cyclized. Early attempts at the enzymatic digestions of lariatin

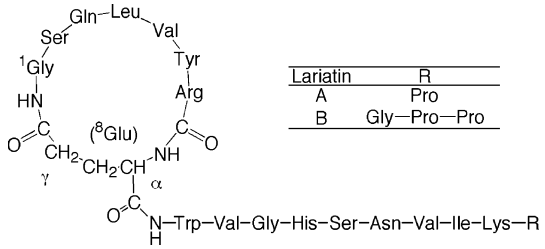

Figure 1. Structures of lariatins A (**1**) and B (**2**).

[†] Kitasato Institute.
[‡] School of Pharmaceutical Sciences.

(1) NIAID's Tuberculosis Antimicrobial Acquisition & Coordinating Facility (TAACF). Web Site, http://www. Taacf.org/about-TB-background.htm (accessed April 10, 2006).
(2) O'Brien, R. J. *Tuberculosis* **2001**, *81*, 1−52.
(3) Iwatsuki, M.; Tomoda, T.; Uchida, R.; Takakusagi, Y.; Matsumoto, A.; Jiang, C. L.; Takahashi, Y.; Arai, M.; Kobayashi, S.; Matsumoto, M.; Omura, S. *J. Antibiot.* **2006**, submitted.

10.1021/ja056780z CCC: $33.50

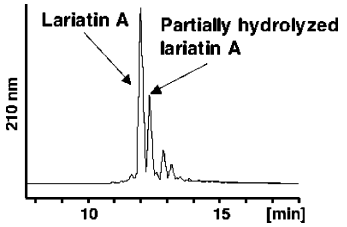

Figure 2. RP−HPLC chart of fragments obtained by limited acid hydrolysis of lariatin A (**1**). HPLC condition: column: Symmetry C18 (2.1ψ x 150 mm), mobile phase: 0−40% acetonitrile (20 min), flow rate: 0.2 mL/minutes, detection: UV 210 nm:

	^{1}Gly-Ser-Gln-Leu-Val-Tyr-Arg-^{8}Glu-Trp-Val-Gly-His-Ser-Asn-Val- Ile - Lys -Pro
NMR analysis	Gly-Ser-Glx
	Glx-Trp-Val-Gly
	Val- Ile - Lys -Pro
	Leu-Val-Tyr-Arg- Glx
	Ser-Asx
MS/MS analysis	Trp-Val-Gly-His-Ser-Asn-Val- Ile - Lys -Pro (Leu)(Gln)
Sequencer analysis of partial hydrolysate	Ser-Gln-Leu-Val-Tyr-Arg- X_1 - X_2-Val-Gly-His-Ser-Asn-Val- Ile - Lys

Figure 3. Summary of the sequence information on lariatins A (**1**).

A with arginylendopeptidase, acromobacter protease I, V8 protease, endoprotease Asp-N, trypsin, and chymotrypsin failed. Only the use of carboxypeptidase P succeeded, indicating that the α-carboxyl group of the C-terminal amino acid is free. Therefore, to obtain fragments suitable for sequencing, a limited acid hydrolysis (0.1 N HCl, 108 °C, 1.5 h) was carried out, yielding several fragments which could be isolated by RP-HPLC (Figure 2). One of the fragments was sequenced as Ser-Gln-Leu-Val-Tyr-Arg- X_1 -X_2-Val-Gly-His-Ser-Asn-Val-Ile-Lys; $X_{1,2}$ not determined. Thus, the linear sequence was concluded to be Gly-Ser-Gln-Leu-Val-Tyr-Arg-Glu-Trp-Val-Gly-His-Ser-Asn-Val-Ile-Lys-Pro. Taking the sequence (Figure 3) and spectral information into consideration, the linear sequence should be cyclized internally between the γ-carboxyl group of Glu8 and the α-amino group of Gly1 and the residue X_1 be a γ-glycylglutamic acid. To confirm this point, the dipeptide was synthesized and the retention time was compared with that of the seventh cycle of the fragment in automated Edman degradation, with the result that residue X_1 was identified as γ-glycylglutamic acid. Furthermore, strong NOESY correlations between Gly1 NH and the side chain protons of Glu8 were observed (Figure 4). Thus, elucidation of the planar structure of lariatin A was completed.

Lariatin B (**2**) had the molecular formula $C_{101}H_{154}N_{29}O_{27}$ established on the basis of NMR and HRFABMS 2205.1568 $[M+H]^+$ (calcd 2205.1568), which was $C_7H_{10}N_2O_2$ larger than that of lariatin A. The ^{1}H and ^{13}C NMR spectra showed the presence of a proline residue and a glycine residue. This was confirmed by an analysis based on complete acid hydrolysis. The MS/MS analysis revealed that the partial sequence of the C-terminal side is Trp-Val-Gly-His-Ser-Asn-Val-Ile-Lys/Glu-Gly-Pro-Pro. Thus, the elucidation of the planar structure for lariatin B was completed, and the sequence Gly-Pro was found to be inserted between Lys and Pro of lariatin A.

Amino acid enantiomers were differentiated by RP-HPLC retention using the *o*-phthalaldehyde method [4] and (*S*)-1-succinimidyl naphthylethylcarbamate method [5] for the primary and secondary amino acids, respectively. These analytical date of lariatins A and B indicated that all the amino acids were of the L-configuration.

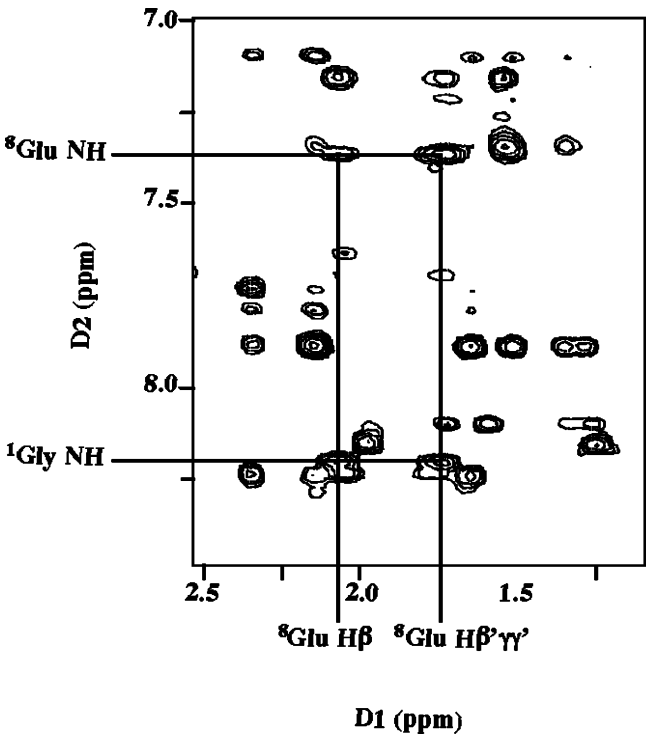

Figure 4. Proof of an internal linkage between the γ-carboxyl group of Glu8 and the α-amino group of Gly1 The strong NOESY correlations between Gly1 NH and the side chain protons of Glu8.

Solution Structure of Lariatin A. Sequence-specific resonance assignments in aqueous solution were made according to the standard method established by Wüthrich and co-workers.[6] The identification of amino acid spin systems was based on DQF−COSY and TOCSY spectra, and complemented the result of NOESY experiments. Figure 5A shows the sequential NOE connectivities observed in the NOESY spectrum with a mixing time of 200 ms, along with ^{3}JNHα and the slowly exchanging amide protons. We have also established the stereospecific assignments of the CβH2 groups by using ^{3}J$\alpha\beta$ coupling constants combined with the intraresidual NH−CβH NOEs observed with a mixing time of 100 ms. ^{3}J$\alpha\beta$ coupling constants were obtained by observing the E.COSY spectrum in D_2O, in which the cross-peaks gave the passive coupling between Cα and Cβ protons. On the basis of the coupling constants and the intensities of intraresidual NOEs, we established the prochiral β-methylene protons and the range of χ_1 side-chain dihedral angles for seven residues, i.e., Ser2 (g^2g^3), Gln3 (t^2g^3), Leu4 (t^2g^3), Tyr6 (t^2g^3), Glu8 (g^2g^3), His12 (t^2g^3), and Asn14 (t^2g^3). For t^2g^3 and g^2g^3 conformations around the Cα-Cβ bond, the χ_1 angle was constrained in the range of $-60 \pm 30°$ and $60 \pm 30°$, respectively. The ^{3}JNHα coupling constants were estimated from the DQF−COSY spectrum in H_2O and converted to the ϕ angle constraints. Ten residues (Ser2, Gln3, Leu4, Val5, Tyr6, Val10, His12, Ser13, Asn14, and Val15) have ^{3}JNHα coupling constants larger than 8 Hz. These ϕ angles were constrained in the range of $-120 \pm 30°$.

(4) Nimura, N.; Kinoshita, T. *J. Chromatogr*. **1986**, *352*, 169−177.
(5) Nimura, N. *Chromatographia* **1987**, *23*, 899−902.
(6) Wüthrich, K *NMR of Proteins and Nucleic Acids*: John Wiley: New York, USA, 1986.

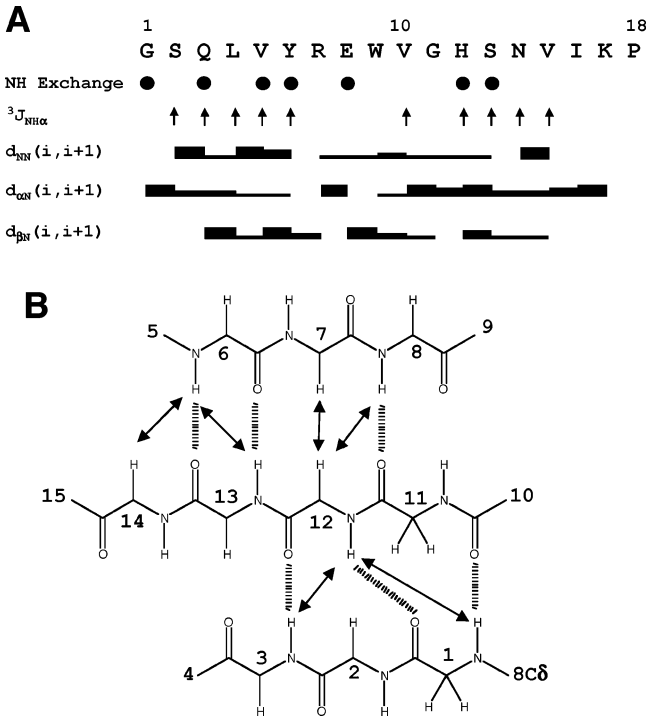

Figure 5. (A) Summary of NOE connectivities, ^{3}JNHα coupling constants and slowly exchanging backbone amide protons observed in lariatin A. The sequential NOEs, dNN(i,i + 1), dαN(i,i + 1), and dβN(i,i + 1) are indicated by bars between two residues. The height of the bars represents the intensities of the NOEs. The values of the coupling constants are indicated by ↑ (>8 Hz) symbols. Slowly exchanging backbone amide protons that are still observed in a TOCSY spectrum recorded after 12 h in D_2O are indicated by filled circles. (B) Hydrogen bond interactions (broken lines) as deduced from amide proton exchange experiment and structure calculations. Key backbone-backbone NOEs are indicated by arrows.

We initially calculated the polypeptide fold by using the distance and dihedral angle constraints. The positions of the hydrogen bonds have been determined on the basis of the preliminary polypeptide fold, along with the results of the amide proton exchange experiments. As a result of this analysis, a total of 6 hydrogen bonds have been identified (Figure 5B), i.e., NH (Gly1) − O (Val10), NH (Gln3) − O (His12), NH (Tyr6) − O (Ser13), NH (Glu8) − O (Gly11), NH (His12) − O (Gly1), and NH (Ser13) − O (Tyr6). Constraints for these hydrogen bonds were added as distance constraints, NH(i)−O(j) and N(i)−O(j), whose target values were set to 1.7 to 2.3 and 2.4 to 3.3 Å, respectively.[7] Finally, a set of 400 individual structures was calculated on the basis of NMR experimental constraints, which consist of 169 distance constraints, 17 dihedral constraints, and 12 hydrogen bond constraints. These calculations provide 81 converged structures, which have no distance violations greater than 0. 2 Å and no dihedral angle violations greater than 5°. Structural statistics for the 81 converged structures are given in Table 1. The deviations from idealized covalent geometry were very small. The Lennard-Jones van der Waals energy was negative, indicating that the nonbonded bad contacts do not exist in the converged structures. For residues Gly1 to Val15, the average pairwise root-mean-square deviation (RMSD) between the 81 individual structures was 0.55 ± 0.20 Å for backbone atoms (N, Cα, C, O) and 1.76 ± 0.38 Å for all heavy atoms.

(7) Gouda, H.; Torigoe, H.; Saito, A.; Sato, M.; Arata, Y.; Shimada, I. *Biochemistry* **1992**, *31*, 9665−9672.

Table 1. Structural Statistics

structural parameter	81 converged structures
RMS deviations from experimental distance constraints (Å)	
all (169)	0.032 ± 0.003
intraresidue (70)	0.034 ± 0.004
sequential (|i − j| = 1) (51)	0.025 ± 0.006
medium range (|i − j| ≤ 5) (12)	0.019 ± 0.009
long range (|i − j| > 5) (36)	0.036 ± 0.006
hydrogen bond (12)	0.036 ± 0.008
RMS deviations from experimental dihedral angle constraints (deg.)[17]	1.154 ± 0.130
energetic statistics (kcal mol^{-1})[a]	
ENOE	9.18 ± 1.65
Etor	1.40 ± 0.32
EL−J	−32.07 ± 6.26
RMS deviations from idealized geometry	
Bonds (Å)	0.004 ± 0.0002
angle (deg.)	0.631 ± 0.034
improper (deg.)	0.410 ± 0.027
average pairwise RMS difference (Å) for Gly1-Val15	
backbone (N, Cα, C, O)	0.55 ± 0.20
all heavy atoms	1.76 ± 0.38

[a] ENOE, Etor, and EL−J are the energies related to the NOE violations, the torsion angle violations, and van der Waals term, respectively. The values of the force constants used for these terms are the standard values as depicted in the X-PLOR 3.1 manual.

These small values clearly indicated that the structure from Gly1 to Val15 is defined very well for all of the 81 individual structures. In a ramachandran-type plots, which are provided as Figure 5S in Supporting Information, the backbone dihedral angles fall in the generally allowed regions. The backbone conformation of Gln3, Tyr6, Arg7, Glu8, His12, and Ser13 is apparently found to be in the β-sheet region. The backbone dihedral angles for both Gly1 and Gly11 are located in the region where only a glycine residue can exist.

Figure 6A shows stereopairs of the best-fit superposition of the backbone atoms for the 81 individual converged structures. The overall structure of lariatin A is characterized by a 'lasso' structure, in which the C-terminal segment (Trp9-Pro18) passes through the ring structure formed by the N-terminal segment (Gly1-Glu8). A small antiparallel β-sheet was identified between Tyr6-Arg7 and His12-Ser13, by considering the backbone ϕ, ψ dihedral angles and the presence of three hydrogen bonds, NH (Tyr6) − O (Ser13), NH (Glu8) − O (Gly11), and NH (Ser13) − O (Tyr6). The sheet is associated with a turn structure involving Glu8-Gly11, which seems to be classified as a type I β-turn. The structure also reveals additional hydrogen bonds on another side of His12-Ser13, i.e., NH (Gly1) − O (Val10), NH (Gln3) − O (His12), and NH (His12) − O (Gly1). These hydrogen bonds seem to stabilize the fold of Gly1-Val15 of lariatin A, i.e., a 'lasso' structure. On the other hand, it appears that the C-terminal residues, Lys17 and Pro18, are highly flexible and disordered in solution, as suggested by the absence of medium- and long-range NOEs. Three main hydrophobic regions are observed on the surface, i.e., the first region involving the side chains of Leu4 and His12, the second one consisting of the side chains of Val5, Tyr6, and Ile16, and the third one formed by the side chains of Trp9 and Val10 (Figure 6B). Interestingly, three residues with polar side chains, Ser2, Gln3, and Asn14, are located on one side of structure of lariatin A (Figure 6C). On the opposite side of the structure, the side chain of Arg7 with a positive charge is positioned.

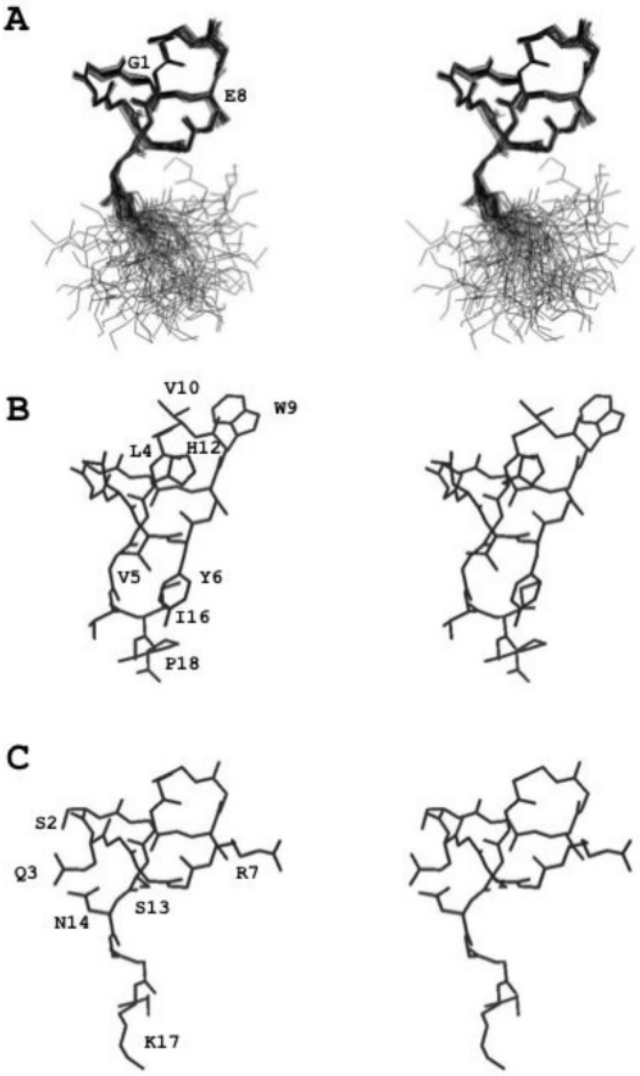

Figure 6. (A) Stereopairs of the superposition of the 81 converged structures of lariatin A. Backbone heavy atoms and those of side chain Glu8 are shown. These are the results of the best fit of the N, Cα, C, and O atoms for Gly1-Val15. (B) and (C) indicate the lowest energy structure of lariatin A. Side-chain atoms of hydrophobic residues (B), and side-chain atoms of hydrophilic residues (C) are shown. Selected residues are labeled with single letter amino acid codes.

Discussion

Lariatins A and B consist of 18 and 20 amino acid residues with a unique internal linkage between the γ-carboxyl group of Glu8 and the α-amino group of Gly1. To date, several peptides which have internal linkages similar to lariatins have been isolated from microbial sources (Figure 7). They can be classified into three groups; anantin, siamycin and lariatin. The anantin type includes anantin,[8] RES-701s,[9] propeptin,[10] and BI-32169,[11] which have an internal linkage between the β-carboxyl group of Asp8 or Asp9 and the α-amino group of Gly1. The siamycin type, including siamycins[12] and aborycin,[13] has an

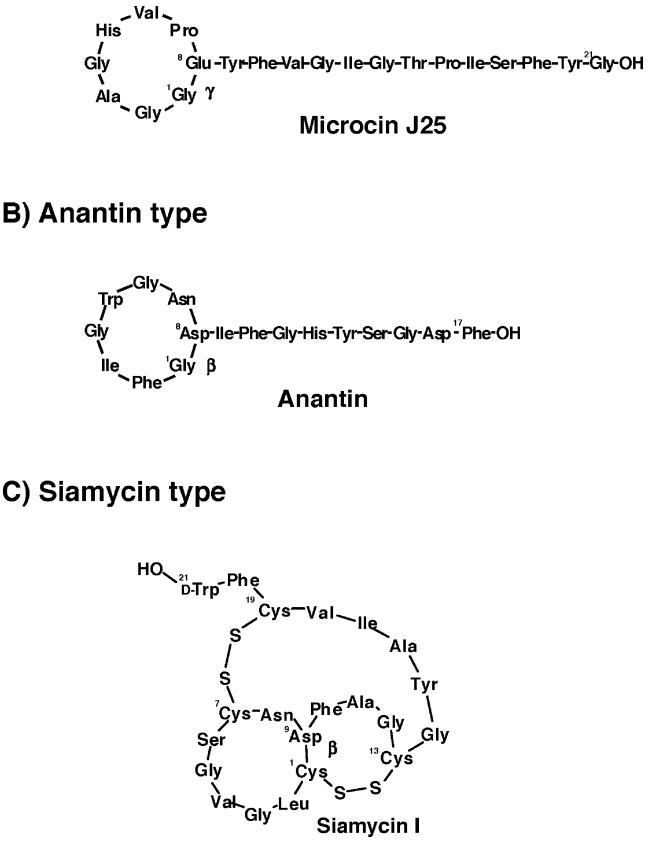

Figure 7. Microbial polypeptides having ring and tail regions.

internal linkage between the β-carboxyl group of Asp9 and the α-amino group of Cys1. They have an additional two disulfide bridges between Cys1 and Cys13, and Cys7 and Cys19. The lariatin type, including lariatins and microcin J25,[14] has an internal linkage between the γ-carboyl group of Glu8 and the α-amino group of Gly1. The structure of microcin J25 was recently revised from head-to-tail circle to head-to-side chain circle.[15,16,17] Anantin, RES-701s, propeptin, BI-32169, and microcin J25 have particular biological functions acting as an atrial natriuretic factor antagonist, endothelin receptor antagonist, prolyl endopeptidase inhibitor, glucagons receptor antagonist, and bacterial RNA polymerase inhibitor, respectively, as predicted from their low similarity at the amino acid level. On the other hand, all siamycin type compounds have anti-HIV activity, as predicted from their high degree of similarity at the amino acid level. Although a linkage between the γ-carboxyl group of Glu8 and the α-amino group of Gly was reported in synthetic peptides,[18] lariatins A and B are the second natural products having such a unique linkage to be reported.

(8) Weber, W.; Fischli, W.; Hochuli, F.; Kupfer, F.; Weibel, E. K. *J. Antibiot.* **1991**, *44*, 164−171.
(9) Morishita, Y.; Chiba, S.; Tsukuda, E.; Tanaka, T.; Ogawa, T.; Yamasaki, M.; Yoshida, M.; Kawamoto, I.; Matsuda, Y. *J. Antibiot.* **1994**, *47*, 269−275.
(10) Kimura, K.; Kanou, F.; Takahashi, H.; Esumi, Y.; Uramoto, M.; Yoshihama, M. *J. Antibiot.* **1997**, *50*, 373−378.
(11) Potterat, O.; Wagner, K.; Gemmecker, G.; Mack, J.; Puder, C.; Vettermann, R.; Streicher, R. *J. Nat. Prod.* **2004**, *67*, 1528−1531.
(12) Tsunakawa, M.; Hu, S. L.; Hoshino, Y.; Detlefson, D. J.; Hill, S. E.; Furumai, T.; White, R. j.; Nishio, M.; Kawano, K.; Yamamoto, S. *J. Antibiot.* **1995**, *48*, 433−434.
(13) Helynck, G.; Dubertret, C.; Mayaux, J. F.; Leboul, J. *J. Antibiot.* **1993**, *46*, 1756−1757.
(14) Salomon, R. A.; Farias, R. N. *J. Bacteriol.* **1992**, *174*, 7428−7435.
(15) Wilson, K. A.; Kalkum, M.; Ottesen, J.; Yuzenkova, J.; Chait, B. T.; Landick, R.; Muir, T.; Severinov, K.; Darst, S. A. *J. Am. Chem. Soc.* **2003**, *125*, 12475−12483.
(16) Rosengren, K. J.; Clark, R. J.; Daly, N. L.; Goransson, U.; Jones, A.; Craik, D. J. *J. Am. Chem. Soc.* **2003**, *125*, 12464−12474.
(17) Bayro, M. J.; Mukhopadhyay, J.; Swapna, G. V.; Huang, J. Y.; Ma, L. C.; Sineva, E.; Dawson, P. E.; Montelione, G. T.; Ebright, R. H. *J. Am. Chem. Soc.* **2003**, *125*, 12382−12383.

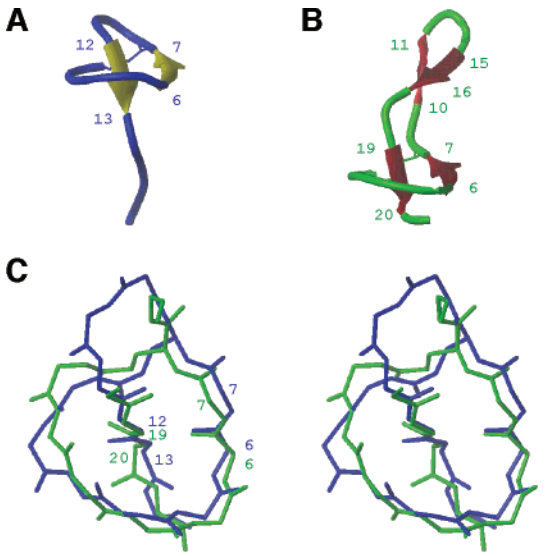

Figure 8. Comparison of the structure of lariatin A (A) with that of microcin J25 (B). The β-sheets are shown with yellow (lariatin A) and red (microcin J25) arrows. (C) Stereopair of the superposition of the ring structures of lariatin A (blue) and microcin J25 (green). This is the result of the best fit of the N, Cα, C, and O atoms for residues 1−8. The view of C is obtained by 70° rotation of A and B around horizontal axis. Selected residues are labeled with residue numbers.

The three-dimensional structures of RES-701−1, aborycin, and microcin J25 in DMSO-d_6 were reported by Katahira et al.,[19] Frechet et al.[20] and K. A. Wilson et al.,[15] respectively. According to their studies, these peptides undergo the same extraordinary folding, i.e., the 'tail' passes through the 'ring' to form a 'lasso' structure, despite their completely different amino acid sequences, and the lasso structure may be responsible for their biological activities and their resistance to digestion by protease. Lariatins A and B are also resistant to proteases and folded into a 'lasso' structure. In Figure 8A and 8B, the structure of lariatin A is compared with that of microcin J25. Both lariatin A and microcin J25 possess a 'lasso' structure, in which the C-terminal segment passes through the ring structure formed by the N-terminal segment. The overall molecular shape of lariatin A seems to be visually similar to that of microcin J25. However, microcin J25 has an additional antiparallel β-sheet between Val10-Gly11 and Pro15-Ile16. Further, only a few residues (Phe19-Gly21) of the C-terminal segment pass through the ring structure in microcin J25, although seven residues (His12-Pro18) do so in lariatin A. On the other hand, Figure 8C shows the superimposition with respect to the backbone atoms of the ring structures. It revealed the significant overlap between the two backbone conformations. In fact, the RMSD between the two structures is 1.74 Å for the backbone atoms of the ring structure. In addition, the antiparallel β-sheet between part of the ring and the penetrating C-terminal segment is conserved in both lariatin A and microcin J25, i.e., Tyr6-Arg7 and His12-Ser13 of lariatin A correspond to Val6-Pro7 and Phe19-Tyr20 of microcin J25, respectively. These results indicate that lariatin A and microcin J25 have a similar molecular folding with respect to the ring structure, despite their low similarity in amino acid sequence except for Gly1 and Glu8. Interestingly, Gly1 of microcin J25 seems to have a backbone conformation generally not allowed for other amino acids, as observed in Gly1 of lariatin A. These glycine residues are completely conserved among anantin as well as lariatin type compounds. They could be expected to play an important role in the molecular folding of these two groups.

Mycobacteria have a very unique cell wall structure. From the entire genome sequence,[21] there are a number of enzymes involved in the biosynthesis of the cell wall. For example, mycolic acids, extremely long fatty acids, form a broad family of more than 500 closely related structures and comprise about 30% of the dry weight of *M. tuberculosis*, and the microorganism has about 250 distinct enzymes involved in fatty acid metabolism (vs 50 for *E. coli*.). Isoniazid and ethambutol are first line antituberculous drug, which inhibit cell wall biosynthesis; isoniazid inhibits the production of mycolic acid by blocking Type II fatty acid synthase, and ethambutol inhibits that of arabinogalactan mycolate by blocking arabinosyl transferase. Interestingly, these two drugs show specific inhibition of mycobacterial growth. Lariatins exhibit similar biological characteristics, although they inhibited the growth strongly in *M. smegmatis* and weakly in *M. tuberculosis*.[3] Therefore, it is plausible that the target of lariatins lies within the cell wall in mycobacteria.

Three main hydrophobic regions on the surface, the side chains of Leu4 and His12, of Val5, Tyr6, and Ile16, and of Trp9 and Val10 (Figure 6B), three residues on one side with polar side chains, Ser2, Gln3, and Asn14 (Figure 6C) and the side chain of Arg7 with a positive charge on the opposite side is observed. As shown in Figure 6, the hydrophobic regions and the polar residues are distributed uniquely on the lariatin molecule.

Experimental Section

The details of taxonomy and fermentation of this strain and isolation, phyisico-chemical properties and biological activities of lariatins will be published elsewhere.[3]

Analytical Procedure. The mass spectra were measured with a JEOL JSM-700 MS station and a JEOL JSM-AX 505 HA in thioglycetol and a PE Bio systems ESI-Q-TOF-MS by direct injection into an electrospray interface. IR spectra were run in KBr on a HORIBA FT-210. The UV spectra were recorded on a HITACHI 340. The optical rotations were measured on a JASCO DIP-1000 Digital Polarimeter with a 5 cm cell. The melting points were measured on a Yanagimoto Micro Melting Point Apparatus MP−S3. The NMR spectra were measured on a Varian UNITY 400 and a Varian INOVA 600 in methanol-d_4, and peak positions are expressed in parts per million (ppm) based on the reference of methanol peak at δ 3.30 ppm for ^{1}H NMR and δ 49.0 ppm for ^{13}C NMR.

Amino Acid Analysis. Lariatins A and B (50 μg) were completely hydrolyzed in a gas phase of 6N HCl (990 μL) and phenol (10 μL) at 150 °C for 5 h in a reaction vial in which air was replaced by N_2 gas using the Pico-Tag work station (Waters). In the amino acid analysis, the hydrolysates were added to 20 μL of alkalization reagent (ethanol: water: triethylamine = 2:2:1) and dried up in vacuo. The hydrolysates were derivatized with 50 μL of derivatization reagent (ethanol: water: triethylamine: phenyl isothiocyanate = 7:1:1:1) at room temperature for 20 min and dried up in vacuo. The PTC-derivative amino acids were analyzed by HPLC on a Pico-Tag column (3.9 × 150 mm, Waters)

(18) Han, G.; Quillan, J. M.; Carlson, K.; Sadee, W.; Hruby, V. J. *J. Med. Chem.* **2003**, *46*, 810−819.
(19) Katahira, R.; Shibata, K.; Yamasaki, M.; Matsuda, Y.; Yoshida, M. *Bioorg. Med. Chem.* **1995**, *3*, 1273−1280.
(20) Frechet, D.; Guitton, J. D.; Herman, F.; Faucher, D.; Helynck, G.; Monegier du Sorbier, B.; Ridoux, J. P.; James-Surcouf, E.; Vuilhorgne, M. *Biochemistry* **1994**, *33*, 42−50.
(21) Cole, S. T. et al. *Nature* **1998**, *393*, 537−544.

as described. HPLC was carried out using HP-1100 systems (Hewlett-Packard). In the absolute configuration analysis, a reverse phase HPLC analysis of the derivatization of amino acids with *o*-phthalaldehyde[4] or (*S*)-1-succinimidyl naphthylethylcarbamate[5] was applied. Amino acid sequencing was performed on a Shimadzu PPSQ-10 protein sequencer using standard procedure.

Limited acid hydrolysis was performed with 0.1 N HCl at 108 °C for 1.5 h. yielded a fragment which could be isolated by RP-HPLC with a liner gradient of acetonitrile in 0.05% H_3PO_4, and analyzed with the protein sequencer described above.

Synthesis and Identification of γ-Glycylglutamic Acid. The solid-pahse synthesis of γ-glycylglutamic acid was carried out on a Shimadzu PSSM-8 with a standard procedure[22] to condensate *N*-α-9-fluorenylmethoxycarbonylglycine-2-chlorotritylchrolide resin and *tert*-butyl glutamate using benzotriazole-1-yloxytripyrrolidinephosphonium hexafluorophospahte and 1-hydroxybenzotriazole.

The identification was based on HPLC performed under the following conditions: column, Wakosil-PTC column (4.0 × 200 mm, Wako Co.); mobile phase, PTC-AA buffer A and B (Wako Co.), 0−70% (15 min); UV detection at 254 nm; flow rate of 1.0 mL/minute. The PTC derivative of γ-glycylglutamic acid was eluted with a retention time of 2.32 min.

Solution Structure Analysis. The NMR experiment was performed as described below: 1.64 mg of sample was dissolved in 0.4 mL of either 90%H_2O/10%D_2O or D_2O containing 25mM CD_3COONa. The pH of the sample solution was adjusted to 5.0. All NMR spectra were recorded on a Varian INOVA600 spectrometer operating at 600 MHz as the proton frequency at three temperatures, 5, 15, and 25 °C, to obtain unambiguous resonance assignments. For sequential resonance assignments and extraction of structural information, DQF−COSY,[23] TOCSY,[24] NOESY,[25] ROESY[26] and E.COSY[27] experiments were performed in the phase-sensitive mode.[28] DQF−COSY and E.COSY spectra were recorded with 512 increments of 8K data points and 32 transients. TOCSY spectra were recorded with mixing times of 20 and 50 ms. NOESY spectra were obtained with mixing times of 100, 200, and 300 ms at 5 and 15 °C. ROESY spectra were obtained with mixing times of 200 ms at 25 °C and 512 increments of 2K data points were recorded with 32 to 96 transients for TOCSY, NOESY, and ROESY experiments. For the identification of slowly exchanging backbone amide protons, TOCSY spectra were recorded sequentially with a time interval of 60 min in D_2O solution at 5 °C. The solvent resonance was suppressed by selective irradiation during a relaxation delay of 2.0 s. Chemical shifts were referenced with respect to H_2O, which in turn was calibrated using an internal standard, 2,2-dimethyl-2-silapentane-5-sulfonate (DSS), in a different sample. Chemical shift values of 4.95, 4.85, and 4.75 ppm for water signal were used at temperatures 5, 15, and 25 °C, respectively. The structure calculation was performed as described below: Interproton distance constraints were obtained from the NOESY spectra. All NOE cross-peaks that could be observed in the NOESY spectrum with a mixing time of 100 ms were integrated in order to derive proton−proton distance constraints. The NOESY spectrum acquired at mixing times of 200 and 300 ms was used to confirm that the weak NOE cross-peaks in the 100-ms spectrum were not noises. Volumes of the five nonoverlapping geminal β-proton cross-peaks were averaged and used for calibrating measured NOE volumes. A distance of 1.8 Å was used as a reference for geminal β-proton cross-peaks. This calibration yielded the theoretically expected values, 2.5 Å, for the distances between the neighboring ring-protons of Trp9. Distance constraints were classified into four categories corresponding to 1.8−2.5, 1.8−2.8, 1.8−3.5, and 1.8−5.0 Å. Pseudoatoms were applied to the upper bounds of degenerate of unassigned methylene, methyl and aromatic ring groups.[29] In addition, 0.5 Å was added to the distance constraints involving methyl protons. All calculations were performed on a Silicon Graphics OCTANE workstation with the program X-PLOR.[30] The dynamical simulated annealing protocols were used in order to calculate three-dimensional structures. The standard force field parameter set (parallhdg.pro) and topology file (topallhdg.pro) were used. The starting structures with a random array of atoms were regularized by the dgsa.inp protocol;[31,2] then the refine.inp protocol was used for optimization of structures.[33] Finally, the restrained minimization was performed using the standard Lennard−Jones van der Waals energy function, which was not used in the dynamical simulated annealing calculations. NOE distance and dihedral angle constraints were applied with 50 kcal mol^{-1} $Å^{-2}$ and 200 kcal mol^{-1} rad^{-2} force constants, respectively.

Acknowledgment. This study was supported in part by the grant of the 21st Century COE Program and Scientific Research on Priority Areas 16073215 from the Ministry of Education, Culture, Sports, Science and Technology, Japan. We would like to thank Prof. Tadashi Yasuhara of the Junior College Department, Tokyo University of Agriculture for amino acid sequence analysis, Prof. Hiroshi Honma of the School of Pharmaceutical Sciences, Kitasato University for determination of the absolute configuration of amino acids, and Prof. Daisuke Uemura of the Department of Chemistry, Nagoya University for ESI−MS/MS mesurements.

Supporting Information Available: NMR data of lariatins A and B, ramachandran-type plots, restraint data for determination of lariatin A's solution structure, it's coordinates list and complete ref 21. This material is available free of charge via the Internet at http://pubs.acs.org.

JA056780Z

(22) Chang, C. D.; Meienhofer, J. *Int. J. Pept. Protein. Res.* **1978**, *11*, 246−249.
(23) Rance, M,; Sørensen, O. W.; Bodenhausen, G.; Wagner, G.; Ernst, R. R.; Wüthrich, K. *Biochem. Biophys. Res. Commun.* **1983**, *117*, 479−485.
(24) Bax, A. D.; Davis, D. G. *J. Magn. Reson*. **1985**, *65*, 355−360.
(25) Macura, S.; Huang, Y.; Suter, D.; Ernst, R. R. *J. Magn. Reson*. **1981**, *43*, 259−281.
(26) Bax, A.; Davis, D. G. *J. Magn. Reson*. **1985**, *63*, 207−213.
(27) Griesinger, C.; Sørensen, O. W.; Ernst, R. R. *J. Magn. Reson*. **1987**, *75*, 474−492.
(28) States, D. J.; Haberkorn, R. A.; Ruben, D. J. *J. Magn. Reson*. **1982**, *48*, 286−292.
(29) Wüthrich, K.; Billeter, K.; Brawn, W. *J. Mol. Biol*. **1983**, *169*, 949−961.
(30) Brünger, A. T. *X-PLOR Manual Version 3.1*; Yale University: New Haven, CT, **1993**.
(31) Nilges, M.; Clore, G. M.; Gronenborn, A. M. *FEBS Lett*. **1988**, *229*, 317−324.
(32) Nilges, M.; Clore, G. M.; Gronenborn, A. M. *FEBS Lett*. **1988**, *239*. 129−136.
(33) Nilges, M.; Kuszewski, J.; Brunger, A. T. *Computational Aspects of the Study of Biological Macromolecules by NMR*; Plenum Press: New York, USA, 1991.